

From Nonequilibrium to Equilibrium: Insights from a Two-Population Occupation Model

Jérôme Garnier-Brun,^{1,2,*} Ruben Zakine,^{2,3,*} and Michael Benzaquen^{2,3,4}

¹*Department of Computing Sciences & Department of Finance, Università Bocconi, Milan, Italy*

²*Chair of Econophysics and Complex Systems, École Polytechnique, 91128 Palaiseau Cedex, France*

³*LadHyX UMR CNRS 7646, École Polytechnique, 91128 Palaiseau Cedex, France*

⁴*Capital Fund Management, 23 Rue de l'Université, 75007 Paris, France*

(Dated: December 20, 2024)

In socioeconomic systems, nonequilibrium dynamics naturally stem from the generically non-reciprocal interactions between self-interested agents, whereas equilibrium descriptions often only apply to scenarios where individuals act with the common good in mind. We bridge these two contrasting paradigms by studying a Sakoda-Schelling occupation model with both individualistic and altruistic agents, who, in isolation, follow nonequilibrium and equilibrium dynamics respectively. We investigate how the relative fraction of these two populations impacts the behavior of the system. In particular, we find that when fluctuations in the agents' decision-making process are small (high rationality), a very moderate amount of altruistic agents mitigates the sub-optimal concentration of individualists in dense clusters. In the regime where fluctuations carry more weight (low rationality), on the other hand, altruism progressively allows the agents to coordinate in a way that is significantly more robust, which we understand by reducing the model to a single effective population studied through the lens of active matter physics. We highlight that localizing the altruistic intervention at the right point in space may be paramount for its effectiveness.

Equilibrium statistical mechanics describes the collective behavior of a large number of constituents when their dynamics are driven by the minimization of a globally defined energy. In many complex systems, however, finding such a system-wide objective function may be impossible. This is notably the case e.g. in active matter [1–4], where particles locally inject energy and momentum in the medium, or else in neural networks [5–7], in which non-reciprocal interactions are commonly assumed. Another wide class of problems where finding a global quantity to be minimized is challenging, if not impossible, is socioeconomic systems. Indeed, most often one cannot assume that individuals share a common “utility” they all strive to optimize; it seems more realistic to consider agents as individualistic actors seeking to improve their own satisfaction, possibly at the expense of the wider population, see e.g. [8, 9] for discussions on this issue. In this context, Zakine *et al.* [10] notably showed that in an occupation model where a fixed number of individualistic agents populate a lattice depending on their *own* preference, detailed balance is violated at the “microscopic” level, and this regardless of the details of the agent’s decision rules. Coarse-graining the system, the density of agents follows a stochastic hydrodynamic equation in which the driving term cannot be written as a gradient of a free energy functional, placing the system out of equilibrium [11, 12].

Human behavior is inherently intricate, however, therefore considering agents as purely and unanimously selfish may prevent one from correctly modeling the complex interactions between individuals, and importantly rules out the potential influence of a central planner. In this Letter, we address these limitations by considering the interaction between individualistic and altruistic agents, who maximize the system-wide aggregate utility instead of their own. By placing ourselves in a context where an isolated system of individualists follows nonequilibrium dynamics, our model notably extends the re-

sults of Grauwin *et al.* [13] and Jensen *et al.* [14] (see below). Having uncovered the salient effect of altruism in our two-population setting, we then introduce a “well-mixed” approximation of our model, comprising of a single population making their decision based either on their personal satisfaction or on the collective well-being with a given probability. This reduced setting allows us to leverage recent advances in the theory of active matter, namely the so-called generalized thermodynamic mapping [15, 16], thereby providing a physical interpretation of the effect of altruism through the change of properties of the “liquid” of agents. Beyond our socioeconomic-inspired setting, our results contribute to the ongoing effort towards the better understanding of the effect of non-reciprocal interactions in complex systems [17–23].

Model. Suppose an individual is endowed with a utility function u . This utility function is a measure of their satisfaction at a position $x \in [0, L]^d$ in, say, a city, and reads

$$u(\phi(x)) = -|\phi(x) - \rho^*|^\gamma, \quad \gamma > 0 \quad (1)$$

where $\phi(x)$ is a locally perceived density of neighbors, and $0 < \rho^* < 1$ is the community-wide ideal of surrounding occupation density [24]. The perceived density is given by $\phi(x) \equiv \phi([\rho], x) = (G * \rho)(x)$, where the density kernel G of standard deviation σ is generically expected to decrease monotonically, while $\rho(x)$ is simply the population density field in this idealized world. As the utility function $u(z)$ described in Eq. (1) is non-monotonic, our toy model essentially relies on the following assumption: Individuals wish to reside in an area that is not too empty, as they want to enjoy a rich social environment and have access to a number of services, but that is not too full either, in order to benefit from a good quality of life and high level of comfort.

As mentioned above, a common starting point for such a model is to assume that agents behave such as to maximize their own satisfaction, that is the utility function evaluated at

the position they choose to live in. Then, imagine some purely *altruistic* agents who have the common interest in mind when making their decision. In other words, instead of attempting at maximizing their own utility, these agents seek to improve the average outcome of the society, in our case proportional to the *global* utility $\mathcal{U}[\rho] = \int dx u(\phi([\rho], x))\rho(x)$, potentially at the cost of their own satisfaction. If such infinitely benevolent individuals may appear somewhat unrealistic, this behavior could also be seen to arise through the action of a central planner that would have the power to influence the decision of individuals, for instance through social housing.

We now consider the scenario where space is occupied with a conserved global density ρ_0 of agents, split between fixed fractions $1 - \alpha$ of individualistic agents, and α of altruistic agents. This can be modeled with two coexisting and interacting density fields $\rho_I(x, t)$ and $\rho_A(x, t)$, describing the spatial and temporal distribution of individualists and altruists, respectively. We will assume that agents do not care (or equivalently do not know) about the “type” of other agents, e.g. an individualist perceives the presence of another individualist as equivalent to that of an altruist.

Let us start by describing the dynamics followed by the density of individualistic agents. While the evolution equation can be derived from the “microscopic” (local) dynamics of non-overlapping agents on a d -dimensional lattice [10] using a path integral approach [25], we choose, for simplicity, to present the model directly at the coarse-grained level:

$$\partial_t \rho_I = \nabla \cdot \left(M_I[\rho_I, \rho_A] \nabla \mu_I[\rho_I, \rho_A] + \sqrt{2T M_I[\rho_I, \rho_A]} \xi_I \right), \quad (2)$$

with $M_I[\rho_I, \rho_A] = \rho_I(1 - \rho_A - \rho_I)$ a standard non-overlapping motility, ξ_I a Gaussian white noise in space and time, and μ_I an effective chemical potential,

$$\mu_I[\rho_I, \rho_A] = T \log \left(\frac{\rho_I}{1 - \rho_I - \rho_A} \right) - u(\phi([\rho_I + \rho_A], x)). \quad (3)$$

The first term is an entropic contribution (i.e. diffusion of the density field), with T a temperature parametrizing the fluctuations in the decision-making process of the agents. This is rather standard in the socioeconomic literature [8, 26], where the inverse temperature is referred to as the “rationality”, or more precisely as the “intensity of choice”. The second term can be understood as a consequence of agents maximizing their utility (cleverly coined “utility-taxi” in [27]). Importantly, we showed in [10] that a utility function that is nonlinear in the perceived density ϕ *cannot* be written as the functional derivative of a global functional of the density field. As a result, the steady-state solution of Eq. (2) may not be described with the standard tools of equilibrium statistical mechanics. Let us stress that this is where our model significantly differs from that of Refs. [13] and [14]. Indeed, both these seminal works leveraged a predefined district-based construction that allows a system of individualists to minimize an effective free energy. Yet, the existence of such an object in socioeconomic systems is likely the exception rather than the

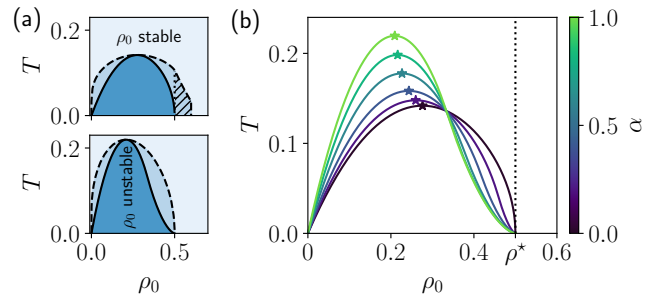


FIG. 1. (a) Phase diagrams in the $\alpha = 0$ (top) and $\alpha = 1$ (bottom) cases with $\gamma = 3/2$ and $\rho^* = 1/2$, full lines indicating the spinodals, and dashed lines delimiting the binodal region where the homogeneous state is metastable. In the hatched area, concentration is possible despite $\rho_0 \geq \rho^*$. (b) Spinodal curves for different α .

rule [8]; assessing the robustness of results to an inherently nonequilibrium setting is therefore an important question.

Altruists, on the other hand, follow the dynamics

$$\partial_t \rho_A = \nabla \cdot \left(M_A[\rho_A, \rho_I] \nabla \frac{\delta \mathcal{F}}{\delta \rho_A} + \sqrt{2T M_A[\rho_A, \rho_I]} \xi_A \right), \quad (4)$$

with $M_A[\rho_A, \rho_I] = \rho_A(1 - \rho_A - \rho_I)$, ξ_A a Gaussian white noise, and where now $\mathcal{F}[\rho_I, \rho_A] = -\mathcal{U}[\rho_I, \rho_A] + T\mathcal{S}[\rho_I, \rho_A]$ is a standard free energy functional, sum of the (minus) global utility, and of the entropy of mixing $\mathcal{S}[\rho_I, \rho_A] = \int \{\rho_I \log \rho_I + \rho_A \log \rho_A + (1 - \rho_A - \rho_I) \log(1 - \rho_A - \rho_I)\}$. The coupled Eqs. (2) and (4), together with a prescribed initial density field, describe our *non-reciprocal* hydrodynamic model [28]. When $\alpha = 1$ and there are no individualists, the above equation corresponds to equilibrium dynamics.

Impact of altruism. Before getting into the description of the model when $\alpha > 0$, let us summarize the phenomenology of the $\alpha = 0$ field theory describing purely individualistic agents, as detailed in [10]. In a nutshell, for small temperatures (high rationality), agents aggregate in dense suboptimal clusters. At the mean-field level, that is neglecting the noise in the hydrodynamic equation, the spinodal and binodal curves can respectively be determined analytically through the linear stability analysis of the homogeneous state $\rho(x, t) = \rho_0$, and through the generalized thermodynamics approach introduced in [15, 16]. The resulting phase diagram is shown in Fig. 1(a), top panel [29]. Strikingly, the binodal curve extends to $\rho_0 > \rho^*$: Due to the individualistic nature of the agents, coordination fails and the system ends up in significantly suboptimal concentrated states even when a homogeneous distribution would provide a higher utility on average. A key question is then to determine when and how the introduction of altruism may resolve this counter-intuitive outcome.

We now consider the linear stability of the homogeneous state $\rho_A(x, t) = \alpha \rho_0$ and $\rho_I(x, t) = (1 - \alpha) \rho_0$ in our model. Introducing a small perturbation about this homogeneous state, expanding Eqs. (2) and (4) at leading order and going to Fourier space yields a stability matrix, the eigenvalues of which can be computed analytically, see Supplemental Mate-

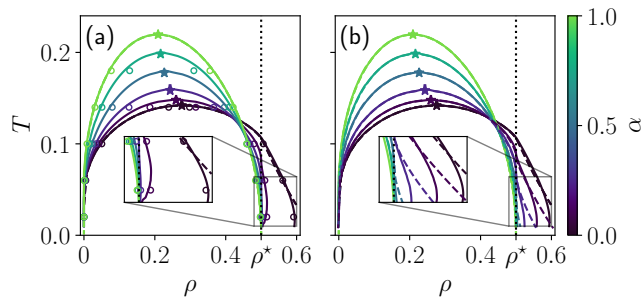


FIG. 2. (a) Binodal curves ($\rho = \rho_A + \rho_I$); markers (o) show numerical estimates of the coexistence densities from agent-based simulations in $d = 2$ (SM). (b) Binodal curves in the case of an effective single-agent population. Dashed lines show the analytic computation using the free energy for $\alpha = 1$ and the generalized thermodynamics approximation (only available for $\alpha = 0$ in (a)). Solid lines are constructed from the numerical resolution of the noiseless hydrodynamic PDEs with Gaussian G , $\sigma = 10$, $L = 1000$.

rial (SM). Spinodal curves for $\alpha > 0$ are shown in Fig. 1(b). A first important observation is that in the vicinity of $\rho_0 = \rho^* = 1/2$, a reasonable fraction of altruists leads the spinodal to lie very close to the equilibrium $\alpha = 1$ curve, leading to quasi-overlapping spinodals for $\alpha \gtrsim 1/2$. For smaller values of ρ_0 , we observe a significant rise in the temperature of the critical point, corresponding to the maximum of the spinodal curves, as α is increased. In other words, the introduction of altruism allows agents to coordinate in a way that is more robust to random fluctuations. Now, below the critical temperature, we expect a metastable region, delimited by binodal curves, which we must now determine in order to properly describe the phase separation of the system in dense and near-empty regions.

We start with the limiting case $\alpha = 1$ (fully altruistic) corresponding to equilibrium dynamics, see above. As a result, the binodal curve can be straightforwardly determined from the free energy density. Within the bulk of the assumed “liquid” (dense) and “gas” (close to empty) phases of the system, the local free energy density is $f(\rho) = -\rho u(\rho) + T[\rho \log \rho + (1 - \rho) \log(1 - \rho)]$. Performing the double-tangent construction (or equivalently the Maxwell construction) on this function, yields the coexistence densities of the system for a given couple (ρ_0, T) , thereby delimiting the binodal. The resulting phase diagram in this $\alpha = 1$ case is shown in Fig. 1(a), bottom panel. Importantly, one can see that it does not go beyond $\rho = \rho^*$, meaning that, as expected, the system no longer sub-optimally concentrates when a uniform distribution of agents is preferable.

What happens for intermediate values of α ? While the coupled nature of the dynamics prevents us from answering this question analytically, a simple alternative is to set the initial total density ρ_0 to its critical value obtained from linear stability analysis, and to numerically solve the system of noiseless partial differential equations (PDE) while varying temperature. The densities measured in the bulk of the liquid

and gas phases of the solutions then give a numerical estimate of the two branches of the binodal, which we show in Fig. 2(a). We verify that in the $\alpha = 1$ case, these densities perfectly match the equilibrium theoretical result. In addition to this numerical resolution at the coarse-grained level, we have also performed agent-based numerical simulations on two-dimensional lattices, see SM for details. The coexistence densities measured from these simulations are shown by the markers on Fig. 2(a), displaying an excellent match with the mean-field predictions. In our model, the effectiveness of the mean-field equations can be understood through the smoothing induced by the kernel G , which averages out fluctuations in the chemical potentials.

Altruism appears to have two markedly distinct effects on the binodals of the system. (i) At low temperatures, a minute fraction of altruistic agents has a very strong effect on the aggregate behavior of the system. As shown in the inset of Fig. 2(a), small values of α indeed lead the agents to collectively behave as if the global utility was the quantity optimized by all agents, and almost immediately kill the sub-optimal concentration at densities $\rho > \rho^*$ of the fully individualistic population. This very strong effect when T is small, which appears to be compatible with the “catalytic” effect of altruism described in Ref. [14] in a different setting, can be understood by observing the spatial distribution of the two types of agents. As visible in the agent-based simulation shown in Fig. 3(a), altruistic agents can very effectively inhibit the concentration of individualists by placing themselves at the boundary of population clusters, triggering a progressive spreading of the dense regions and effectively acting as surfactants. (ii) At higher temperatures, and as expected from the critical temperature computed through the linear stability analysis, altruism allows the system to be significantly more robust to fluctuations, and to remain phase separated when it is beneficial for the agents. In this region, the effect of α is much more progressive, and as shown in Fig. 3(b), not particularly localized in space. See SM for an illustration of how these changes in the binodal translate in an improvement of the global utility as α is increased.

Well-mixed approximation. The two-agent model discussed above demonstrates the strong impact of altruism. While we were able to unravel the mechanisms at low temperatures, we failed at describing it analytically beyond linear stability, and at clearly interpreting its effect at higher temperatures. In order to improve our theoretical understanding, let us introduce an alternative version of the model with a single type of agents that happen to be altruistic at times. We now take α to be the probability of being altruistic at a given instant, leaving a $1 - \alpha$ probability to be individualistic (which is in fact similar to the prescription first proposed in [13]). The resulting hydrodynamic equation for the single density field ρ

$$\partial_t \rho = \nabla \cdot \left[M[\rho] \nabla \mu_{\text{wm}}[\rho] + \sqrt{2TM[\rho]} \xi \right], \quad (5)$$

with $M[\rho] = \rho(1 - \rho)$, $\mu_{\text{wm}}[\rho] = (1 - \alpha)\mu_I[\rho_I = \rho, \rho_A = 0] + \alpha\delta\mathcal{F}/\delta\rho$ that interpolates between individualist and altruist chemical potentials, $\mathcal{F}[\rho] = -\mathcal{U}[\rho] + T \int [\rho \log \rho + (1 -$

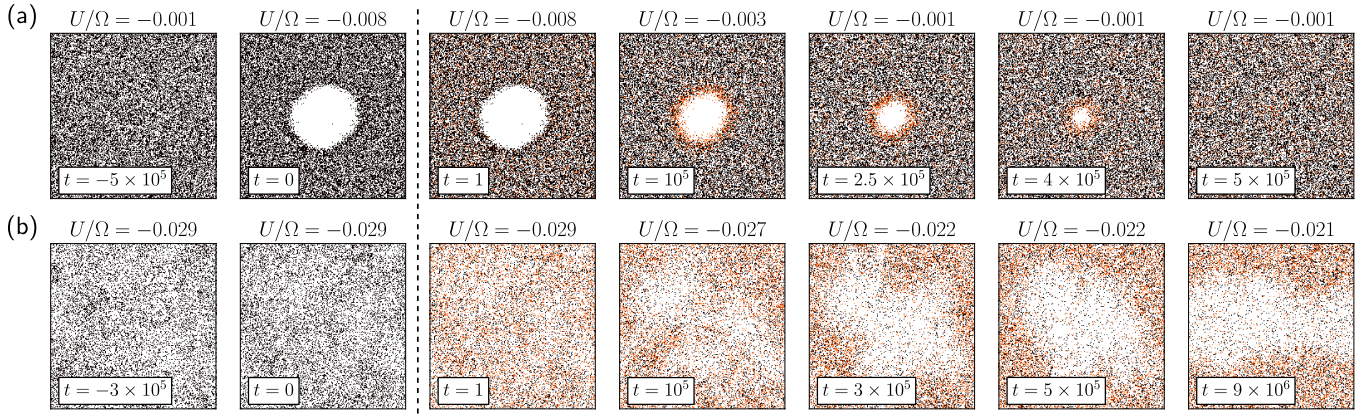


FIG. 3. Illustration of the effects of altruists in an agent-based simulation of our model, see SM. In a system of size $\Omega = L \times L$, with $L = 200$, of $N = \lfloor \rho_0 L^2 \rfloor$ individualists (black) are left to evolve from an initially homogeneous configuration. After 5×10^5 iterations (vertical dashed line), a randomly selected fraction α individualists are replaced with altruists (red). (a) $\rho_0 = \rho^* = 1/2$, $T = 0.04$, $\alpha = 0.12$ (phase separation is unfavorable); (b) $\rho_0 = 0.26$, $T = 0.14$, $\alpha = 0.5$ (phase separation is favorable). For both, G is Gaussian with $\sigma = 7$, $\gamma = 3/2$ and $\rho^* = 1/2$.

$\rho) \log(1 - \rho)]$. By design, this simplified model coincides with the original two-agent version in the extremal $\alpha = 0$ and $\alpha = 1$ cases. In fact, both prescriptions are equivalent provided these two populations are well mixed in space, that is assuming $\frac{\rho_A(x)}{\rho_I(x)} = \frac{\alpha}{1-\alpha} \forall x$, which appears to be the case at sufficiently high temperature, see Fig. 3(b). By definition, this condition is verified in the homogeneous state where the density is uniform. Therefore both models have the same critical point and spinodal curves for a given value of α , see SM.

The binodal curves in this setting can again be computed by numerically solving the PDE of Eq. (5). The resulting coexistence densities are shown as solid lines in Fig. 2(b). In the higher temperature region, the correspondence between the two models is quite remarkable, confirming that this simplified description may serve its purpose for the understanding of the role of altruism in the vicinity of $T_c(\alpha)$. For small T , the outcomes of the two prescriptions differ, as can be expected from the spatially localized action of altruistic agents that breaks down the “well-mixed” assumption, see Fig. 2 and Fig. 3(a).

Now, having a single scalar density field ρ is very convenient as it allows us to employ a generalized thermodynamics construction [15, 16] after performing a gradient expansion of the chemical potential in Eq. (5): $\mu_{\text{wm}}([\rho], x) = \mu_0(\rho) + \lambda(\rho)(\nabla\rho)^2 - \kappa(\rho)\nabla^2\rho + O(\nabla^4)$. Taking the kernel G to be Gaussian of range σ yields explicit expressions for $\mu_0(\rho)$, $\kappa(\rho)$ and $\lambda(\rho)$, see SM. The gradient expansion then suggests a bijective change of variable $R(\rho)$ with $\kappa(\rho)R''(\rho) = -[\kappa'(\rho) + 2\lambda(\rho)]R'(\rho)$ [15, 16], which restores locality in the phase properties and allows one to perform a double-tangent construction on a new generalized free energy density $g(R)$, defined such that $\mu_0(R) = \frac{dg}{dR}$. Using Eq. (1) yields a (lengthy) analytical expression for $\mu_0(R)$, see SM. The predicted binodal densities are shown with dashed lines in Fig. 2(b). In the region of interest (upper part of the binodals), the match between the generalized thermodynamics analytical

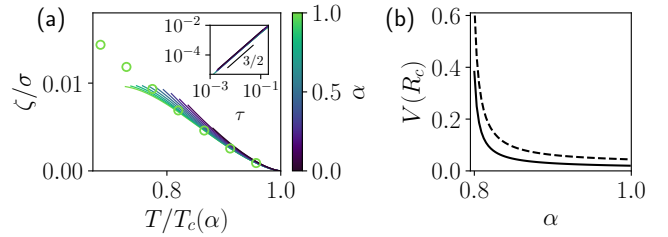


FIG. 4. (a) Normalized pseudo tension ζ/σ (solid lines) as a function of rescaled temperature $T/T_c(\alpha)$, for different α . Markers (\circ) indicate the true surface free energy in the equilibrium case $\alpha = 1$. Inset: the tension follows the mean-field critical scaling $\zeta \propto \tau^s$ with $\tau = 1 - T/T_c(\alpha)$ and $s = 3/2$ [31, 32]. (b) Value of the quasi-potential $V(R_c)$ computed for fixed ρ_0 , $T = 0.18$ and close to the $\alpha = 0.8$ binodal. Solid line: close to the gas density $\rho_0 = \rho_g(T) + \epsilon$. Dashed line: close to the liquid density $\rho_0 = \rho_\ell(T) - \epsilon$, with $\epsilon = 10^{-3}$.

results and the numerically solved PDEs is excellent [30].

Surface tension and nucleation. Having verified the adequacy of the well-mixed approximation and of the gradient expansion close to the critical temperature, we leverage this analytically tractable setting to improve our understanding of the influence of altruism in this region. We notably propose to quantify the typical waiting times before observing a phase change as altruism is varied. Indeed, in the binodal regions the nucleation rate, which governs the time required for the agents to trigger phase separation, is ultimately α dependent.

The nucleation probability \mathbb{P} (or nucleation rate) in active fluids was recently shown to follow classical nucleation theory [33]. It satisfies a large deviation principle $\log \mathbb{P} \sim -V(R_c)/T$ for small T , where the quasi-potential $V(R_c)$ represents the cost to escape the homogeneous state and reach a critical nucleus (a bubble of gas or a droplet of liquid) of radius R_c , which then drives the system to complete phase separation. The quasi-potential $V(R_c)$ crucially depends on the surface tension, on the gas and liquid densities, and on the sat-

uration (i.e. where we lie in the binodal). The surface tension of nonequilibrium liquids is a versatile quantity that should be interpreted with care [34–36]. This being said, the pseudo-tension obtained from the thermodynamic mapping [15, 16] has been shown to regulate Ostwald ripening and therefore the fate of nucleation events in scalar active field theories [33, 37].

The pseudo-tension ζ we compute from the gradient expansion (see SM) is shown for various α in Fig. 4(a). For $\alpha = 1$, we verify that the tension matches the true interfacial energy measured on a stationary profile close to the critical point. With this, one can finally compute the quasi-potential $V(R_c)$ and its dependence on α . For a fixed T [38] and starting close to the binodal densities for, say, $\alpha = 0.8$, one observes a sharp decrease of the quasi-potential as α increases, see Fig. 4(b). Further, since the quasi-potential becomes comparable to T as α increases, the nucleation rate is of order 1, and nucleation can thus no longer be seen as a rare event. These results are in line with the intuition that altruism radically facilitates the nucleation of the phase-separated state when it is beneficial for the agents, see Fig. 3(b).

Concluding remarks. In this work, we have considered a two-population extension of a general Sakoda-Schelling occupation model to study the interaction between individualistic and altruistic agents. We found that when agents are highly rational, i.e. when the temperature in our model is small, a very small fraction of altruistic agents strikingly kills the peculiar aggregation of individualistic agents in sub-optimal dense clusters. This result notably suggests that the nonequilibrium driving caused by individualism in socioeconomic systems does not necessarily lead to an immediate change in a model’s phenomenology. At higher temperatures, altruism drives the system in the phase-separated configuration, which here again optimizes the global utility. In this region, the influence of altruism can be further understood through the lens of the probability of nucleation when adopting an effective single-population version of the model.

Let us finally discuss further the single-population prescription, as it can in fact be considered as a different model in itself. While it is nearly identical to the original two-population prescription close to the critical point, there is a striking difference in the low temperature behavior of the two models, see the inset of Fig. 2(b). This observation can have somewhat important socioeconomic implications. Indeed, it shows that having a small fraction of agents devoted to the maximization of the average welfare is much more effective than having an equivalent fraction of the decisions of identical agents be dictated by the well-being of others. While this result arises in a very simplified setting here, our system provides a clear illustration of the action of a central planner being substantially more effective than leaving individuals the possibility of being philanthropic. Here, this difference can be understood by observing that altruistic agents may concentrate at the boundaries of sub-optimally generated empty spaces to progressively bring back the system to a globally optimal outcome, as illustrated in Fig. 3. In other words, the possibility of localizing the altruistic intervention at the right point in space

is paramount for its effectiveness. It appears sensible to believe that such a conclusion might in fact be quite generic.

Acknowledgments. We thank J.-P. Bouchaud for fruitful discussions. This research was conducted within the Econophysics & Complex Systems Research Chair, under the aegis of the Fondation du Risque, the Fondation de l’École polytechnique, the École polytechnique and Capital Fund Management.

* Both authors contributed equally, alphabetical order.

- [1] S. Ramaswamy, The mechanics and statistics of active matter, *Annu. Rev. Condens. Matter Phys.* **1**, 323 (2010).
- [2] M. C. Marchetti, J.-F. Joanny, S. Ramaswamy, T. B. Liverpool, J. Prost, M. Rao, and R. A. Simha, Hydrodynamics of soft active matter, *Reviews of modern physics* **85**, 1143 (2013).
- [3] J. Stenhammar, A. Tiribocchi, R. J. Allen, D. Marenduzzo, and M. E. Cates, Continuum theory of phase separation kinetics for active Brownian particles, *Physical review letters* **111**, 145702 (2013).
- [4] R. Wittkowski, A. Tiribocchi, J. Stenhammar, R. J. Allen, D. Marenduzzo, and M. E. Cates, Scalar φ^4 field theory for active-particle phase separation, *Nature communications* **5**, 4351 (2014).
- [5] J. Hertz, G. Grinstein, and S. Solla, Irreversible spin glasses and neural networks, in *Heidelberg Colloquium on Glassy Dynamics: Proceedings of a Colloquium on Spin Glasses, Optimization and Neural Networks Held at the University of Heidelberg June 9–13, 1986* (Springer, 1987) pp. 538–546.
- [6] D. Martí, N. Brunel, and S. Ostojic, Correlations between synapses in pairs of neurons slow down dynamics in randomly connected neural networks, *Physical Review E* **97**, 062314 (2018).
- [7] R. Corral López, V. Buendía, and M. A. Muñoz, Excitatory-inhibitory branching process: A parsimonious view of cortical asynchronous states, excitability, and criticality, *Physical Research* **4**, L042027 (2022).
- [8] J.-P. Bouchaud, Crises and collective socio-economic phenomena: simple models and challenges, *Journal of Statistical Physics* **151**, 567 (2013).
- [9] J. Garnier-Brun, J.-P. Bouchaud, and M. Benzaquen, Bounded rationality and animal spirits: A fluctuation-response approach to Slutsky matrices, *Journal of Physics: Complexity* **4**, 015004 (2023).
- [10] R. Zakine, J. Garnier-Brun, A.-C. Becharat, and M. Benzaquen, Socioeconomic agents as active matter in nonequilibrium Sakoda-Schelling models, *Physical Review E* **109**, 044310 (2024).
- [11] C. Nardini, É. Fodor, E. Tjhung, F. Van Wijland, J. Tailleur, and M. E. Cates, Entropy production in field theories without time-reversal symmetry: quantifying the non-equilibrium character of active matter, *Physical Review X* **7**, 021007 (2017).
- [12] J. O’Byrne, Nonequilibrium currents in stochastic field theories: A geometric insight, *Physical Review E* **107**, 054105 (2023).
- [13] S. Grauwlin, E. Bertin, R. Lemoy, and P. Jensen, Competition between collective and individual dynamics, *Proceedings of the National Academy of Sciences* **106**, 20622 (2009).
- [14] P. Jensen, T. Matreux, J. Cambe, H. Larralde, and E. Bertin, Giant catalytic effect of altruists in Schelling’s segregation model,

- Physical Review Letters **120**, 208301 (2018).
- [15] A. P. Solon, J. Stenhammar, M. E. Cates, Y. Kafri, and J. Tailleur, Generalized thermodynamics of phase equilibria in scalar active matter, *Physical Review E* **97**, 020602 (2018).
- [16] A. P. Solon, J. Stenhammar, M. E. Cates, Y. Kafri, and J. Tailleur, Generalized thermodynamics of motility-induced phase separation: phase equilibria, laplace pressure, and change of ensembles, *New Journal of Physics* **20**, 075001 (2018).
- [17] M. Fruchart, R. Hanai, P. B. Littlewood, and V. Vitelli, Non-reciprocal phase transitions, *Nature* **592**, 363 (2021).
- [18] G. G. Lorenzana, A. Altieri, G. Biroli, M. Fruchart, and V. Vitelli, Non-reciprocal spin-glass transition and aging, arXiv preprint arXiv:2408.17360 (2024).
- [19] J. Garnier-Brun, M. Benzaquen, and J.-P. Bouchaud, Unlearnable games and “satisficing” decisions: A simple model for a complex world, *Physical Review X* **14**, 021039 (2024).
- [20] Y. Duan, J. Agudo-Canalejo, R. Golestanian, and B. Mahault, Phase coexistence in nonreciprocal quorum-sensing active matter, arXiv preprint arXiv:2411.05465 (2024).
- [21] Y. Avni, M. Fruchart, D. Martin, D. Seara, and V. Vitelli, Dynamical phase transitions in the non-reciprocal Ising model, arXiv preprint arXiv:2409.07481 (2024).
- [22] A. Garcés and D. Levis, Phase transitions in single species Ising models with non-reciprocal couplings, arXiv preprint arXiv:2411.03544 (2024).
- [23] S. Shmakov, G. Osipychева, and P. B. Littlewood, Gaussian fluctuations of non-reciprocal systems, arXiv preprint arXiv:2411.17944 (2024).
- [24] Henceforth, we shall always assume periodic boundary conditions.
- [25] A. Lefevre and G. Biroli, Dynamics of interacting particle systems: stochastic process and field theory, *Journal of Statistical Mechanics: Theory and Experiment* **2007**, P07024 (2007).
- [26] S. P. Anderson, A. De Palma, and J.-F. Thisse, *Discrete choice theory of product differentiation* (MIT press, 1992).
- [27] D. S. Seara, J. Colen, M. Fruchart, Y. Avni, D. Martin, and V. Vitelli, Sociohydrodynamics: data-driven modelling of social behavior, arXiv preprint arXiv:2312.17627 (2023).
- [28] Note that the coupled hydrodynamic model is necessarily out of equilibrium due to the inherently non-reciprocal nature of the coupling between the two types of agents, and this even if the individualistic chemical potential can be written as the functional derivative of a free energy functional, as pointed out in [14] where the $\alpha = 0$ case is in equilibrium.
- [29] Note that when the smoothing kernel G has a sufficiently large range, the noiseless approximation yields excellent predictions for this model [10].
- [30] At low temperatures, where the well-mixed approximation no longer holds, the generalized thermodynamic mapping breaks down. This was already observed in the $\alpha = 0$ instance studied in [10], and it can be understood from the gradient expansion. Indeed, considering the expression of $\kappa(\rho)$ that regulates interface stability to leading order, the non-monotonicity of the utility function leads to a change of sign of κ at $\rho = \rho^*(\alpha + 1)/(1 - \alpha + 2\alpha\gamma)$, at which point one would require keeping higher order terms to stabilize the liquid-gas interface.
- [31] B. Widom, Surface Tension and Molecular Correlations near the Critical Point, *The Journal of Chemical Physics* **43**, 3892 (1965).
- [32] N. V. Brilliantov, J. M. Rubí, and Y. A. Budkov, Molecular fields and statistical field theory of fluids: Application to interface phenomena, *Phys. Rev. E* **101**, 042135 (2020).
- [33] M. Cates and C. Nardini, Classical nucleation theory for active fluid phase separation, *Physical Review Letters* **130**, 098203 (2023).
- [34] G. Fausti, E. Tjhung, M. E. Cates, and C. Nardini, Capillary interfacial tension in active phase separation, *Phys. Rev. Lett.* **127**, 068001 (2021).
- [35] Y. Zhao, R. Zakine, A. Daerr, Y. Kafri, J. Tailleur, and F. van Wijland, Active Young-Dupré equation: How self-organized currents stabilize partial wetting, arXiv preprint arXiv:2405.20651 (2024).
- [36] L. Langford and A. K. Omar, The mechanics of nucleation and growth and the surface tensions of active matter, arXiv preprint arXiv:2407.06462 (2024).
- [37] E. Tjhung, C. Nardini, and M. E. Cates, Cluster phases and bubble phase separation in active fluids: Reversal of the Ostwald process, *Phys. Rev. X* **8**, 031080 (2018).
- [38] The choice of the temperature requires finding a “sweet spot” where T is large enough for the pseudo surface tension ζ to be demonstrably accurate—that is not too far from $T_c(\alpha)$ (Fig. 4(a))—, while being small enough for the large deviation principle of classical nucleation theory to remain valid. As we are mainly interested in the qualitative evolution of $V(R_c)$ with α , we consider $T = 0.18$ to be adequate here.

SUPPLEMENTAL MATERIAL

Linear stability analysis

Two-population model

We start from the coupled evolution equations

$$\partial_t \rho_A = \partial_x \left(\rho_A (1 - \rho_A - \rho_I) \partial_x \frac{\delta \mathcal{F}}{\delta \rho_A(x)} \right) \quad (S1)$$

$$\partial_t \rho_I = \partial_x (\rho_I (1 - \rho_A - \rho_I) \partial_x \mu_I). \quad (S2)$$

Taking $\rho_A(x, t) = \alpha \rho_0 + \epsilon \tilde{\rho}_A(x, t)$, $\rho_I(x, t) = (1 - \alpha) \rho_0 + \epsilon \tilde{\rho}_I(x, t)$ and expanding the equations up to order ϵ , we have the evolution of the perturbations at the linear order

$$\partial_t \tilde{\rho}_A = T(1 - (1 - \alpha) \rho_0) \partial_x^2 \tilde{\rho}_A + \alpha T \rho_0 \partial_x^2 \tilde{\rho}_I - \alpha \rho_0 (1 - \rho_0) \partial_x^2 [2\tilde{\phi} u'(\rho_0) + \rho_0 u''(\rho_0) G * \tilde{\phi}] \quad (S3)$$

$$\partial_t \tilde{\rho}_I = T(1 - \alpha \rho_0) \partial_x^2 \tilde{\rho}_I + (1 - \alpha) T \rho_0 \partial_x^2 \tilde{\rho}_A - (1 - \alpha) \rho_0 (1 - \rho_0) \partial_x^2 [\tilde{\phi} u'(\rho_0)], \quad (S4)$$

with $\tilde{\phi} = G * (\tilde{\rho}_A + \tilde{\rho}_I)$. In Fourier space, these equations yield the linear system

$$\partial_t \begin{bmatrix} \hat{\rho}_A(k, t) \\ \hat{\rho}_I(k, t) \end{bmatrix} = K \begin{bmatrix} \hat{\rho}_A(k, t) \\ \hat{\rho}_I(k, t) \end{bmatrix}, \quad (S5)$$

with the stability matrix $K =$

$$-k^2 T \begin{pmatrix} (1 - (1 - \alpha) \rho_0) - \alpha \rho_0 (1 - \rho_0) \hat{G}(k) [2u'(\rho_0) + \rho_0 u''(\rho_0) \hat{G}(k)] & \alpha \rho_0 - \alpha \rho_0 (1 - \rho_0) \hat{G}(k) [2u'(\rho_0) + \rho_0 u''(\rho_0) \hat{G}(k)] \\ (1 - \alpha) \rho_0 - (1 - \alpha) \rho_0 (1 - \rho_0) \hat{G}(k) u'(\rho_0) & (1 - \alpha \rho_0) - (1 - \alpha) \rho_0 (1 - \rho_0) \hat{G}(k) u'(\rho_0) \end{pmatrix}. \quad (S6)$$

The eigenvalues can be computed explicitly. They read

$$\lambda_1 = -k^2 T (1 - \rho_0), \quad (S7)$$

$$\lambda_2 = -k^2 (T - \rho_0 (1 - \rho_0) \hat{G}(k) [(1 + \alpha) u'(\rho_0) + \alpha \rho_0 u''(\rho_0) \hat{G}(k)]), \quad (S8)$$

which are always real, and thus seem to indicate that chasing cannot be observed from the homogeneous state (contrary to some cases when combining two individualistic populations with competing goals, as documented in [10]). Clearly, λ_1 will always be negative, and we must therefore consider $\lambda_{\max} = \lambda_2$ to determine the spinodal.

Single population simplification

As mentioned in the main text, it is rather straightforward to convince oneself that the linear stability analysis about the *homogeneous* state is the same in the simplification we propose as in our original model. To check that this is indeed the case, we perform the single population computation here. Starting now from Eq. (5), expanding it in the vicinity of the homogeneous state $\rho(x, t) = \rho_0 + \epsilon \tilde{\rho}(x, t)$ and writing the time evolution of the perturbation in Fourier space, we have

$$\partial_t \hat{\rho}(k, t) = -k^2 (T - \rho_0 (1 - \rho_0) \hat{G}(k) [(1 + \alpha) u'(\rho_0) + \alpha \rho_0 u''(\rho_0) \hat{G}(k)]) \hat{\rho}(k, t). \quad (S9)$$

We immediately recognize that the criterion for linear stability is the same as above.

Agent-based simulations

The main text has focused on the coarsened-grained hydrodynamic description of our models. The locally conserved dynamics assumed that agents evolve locally in space, jumping from one site to some neighboring one. In order to ensure that the central conclusions of our study are robust to variations of this setting, as well as to lie closer to standard socioeconomic modeling, we consider a discrete version of our model with non-local moves, which appear more realistic from a practical standpoint.

At every time step in the simulation, an agent (altruistic or individualistic) is randomly selected from an occupied site on the lattice, and is proposed to move to a randomly selected empty site. The difference in the agent's utility Δv is computed based on the type of agent selected (either global or local), and the move is accepted with probability

$$P(\Delta v) = \frac{1}{1 + e^{-\beta \Delta v}}, \quad (\text{S10})$$

with $\beta = \frac{1}{T}$, ensuring that detailed balance is satisfied in the case of a purely altruistic population. As shown in [10], detailed balance is violated for individualistic agents whenever the utility function is a nonlinear function of the *local* perceived density ϕ , consistent with the non-relaxational nature of the dynamics for $\alpha < 1$. Here, the perceived density is computed by performing a discrete convolution between the kernel G and a binary occupation variable n_i , equal to one if site i is occupied and zero if it is empty. The global utility for a system of size Ω is now defined as

$$U = \sum_{i=1}^{\Omega} n_i u_i, \quad (\text{S11})$$

with u_i the (hypothetical) individual utility of an agent located at the associated site.

To measure the coexistence densities shown in Fig. 2(a) of the main text we initialize two-dimensional systems of width $L = 400$ and height $\ell = 100$ in a phase separated state, forming a slab with a concentrated region in the center. The system is left to evolve and the densities are measured by time-averaging the occupation variables n_i once the system has reached a steady-state. In this experiment, we take G to be a Gaussian kernel with characteristic width $\sigma = 7$, explaining the slight disparities with the one-dimensional noiseless PDE resolutions that may be performed on larger systems lying closer to the true mean-field limit $L \rightarrow \infty$, $\sigma \rightarrow \infty$ with $\sigma/L \rightarrow 0$.

As expected from the results of [10] for the $\alpha = 0$ case, we find a very good agreement between the local hydrodynamics and the non-local simulations.

Generalized thermodynamic mapping

Gradient expansion

The “well-mixed” version of the model considers a single type of agents who interpolates between individualistic and altruistic behavior. The chemical potential thus interpolates between the individualistic chemical potential and the altruistic one. The mean-field equation of motion reads

$$\partial_t \rho = \nabla \cdot [\rho(1 - \rho) \nabla \mu_{\text{wm}}], \quad (\text{S12})$$

with

$$\mu_{\text{wm}} = T \log \left(\frac{\rho}{1 - \rho} \right) - u(\phi) - \alpha \int \rho(y) u'(\phi(y)) G(x - y) dy. \quad (\text{S13})$$

To identify a good change of variable that yields the binodal densities, one expands the chemical potential, and one retains the leading order gradient terms. On thus obtains

$$\mu_{\text{wm}}([\rho], x) = \mu_0(\rho) + \lambda(\rho)(\nabla \rho)^2 - \kappa(\rho) \nabla^2 \rho + O(\nabla^4). \quad (\text{S14})$$

The expansion is generic and can be made explicit for any smoothing kernel G . For simplicity, we assume G to be Gaussian with variance σ^2 , and we identify the different terms:

$$\mu_0(\rho) = -u(\rho) - \alpha \rho u'(\rho) + T \log \left(\frac{\rho}{1 - \rho} \right), \quad (\text{S15})$$

$$\kappa(\rho) = \frac{\sigma^2}{2} [(1 + \alpha) u'(\rho) + 2\alpha \rho u''(\rho)], \quad (\text{S16})$$

$$\lambda(\rho) = -\frac{\sigma^2}{2} \alpha [2u''(\rho) + \rho u'''(\rho)]. \quad (\text{S17})$$

Change of variable

To find the binodal densities, one first defines the bijective change of variable $R(\rho)$ that satisfies $\kappa(\rho)R''(\rho) = -[\kappa'(\rho) + 2\lambda(\rho)]R'(\rho)$, which here reads

$$R''(\rho) = -\frac{(1-\alpha)u''(\rho)}{(1+\alpha)u'(\rho) + 2\alpha\rho u''(\rho)}R'(\rho). \quad (\text{S18})$$

Taking our utility function $u(\rho) = -|\rho - \rho^*|^\gamma$, it turns out we always have

$$\frac{u'}{u''} = \frac{\rho^* - \rho}{1 - \gamma}, \quad (\text{S19})$$

which simplifies the differential equation into

$$R'' = -\frac{(1-\alpha)(1-\gamma)}{(1+\alpha)(\rho^* - \rho) + 2\alpha(1-\gamma)\rho}R'. \quad (\text{S20})$$

This equation has to be solved on two distinct domains before “gluing”. The extremal density is

$$\rho_m = \frac{1}{1 + 2\frac{\alpha}{\alpha+1}(\gamma-1)}\rho^*, \quad (\text{S21})$$

and the solution for $R(\rho)$ reads

$$R(\rho) = C_1(\rho - \rho_m)^\xi \Theta[\rho - \rho_m] + C_2(\rho_m - \rho)^\xi \Theta[\rho_m - \rho], \quad (\text{S22})$$

with $\xi = 1 + \frac{(\alpha-1)(\gamma-1)}{1 + \alpha(2\gamma-1)}$, and the constants C_1 and C_2 have to be adjusted such that R is bijective and differentiable. Interestingly enough, we recover a linear change of variable, i.e. $\xi = 1$ if and only if $\gamma = 1$ (linear utility) or $\alpha = 1$ (global utility). We can always shift R with some constant also. In the other way round, we have:

$$\rho = \rho_m + \text{sign}(R)|R|^{\frac{1}{\xi}} \quad (\text{S23})$$

and now the chemical potential

$$\begin{aligned} \mu_0(R) &= -u(\rho(R)) - \alpha\rho(R)u'(\rho(R)) + T \log(\rho(R)/(1 - \rho(R))) \\ &= \left| \rho_m + \text{sign}(R)|R|^{\frac{1}{\xi}} - \rho^* \right|^\gamma + \alpha\gamma(\rho_m + \text{sign}(R)|R|^{\frac{1}{\xi}}) \text{sign}\left(\rho_m + \text{sign}(R)|R|^{\frac{1}{\xi}} - \rho^*\right) \left| \rho_m + \text{sign}(R)|R|^{\frac{1}{\xi}} - \rho^* \right|^{\gamma-1} \\ &\quad + T \log\left(\frac{\rho_m + \text{sign}(R)|R|^{\frac{1}{\xi}}}{1 - \rho_m - \text{sign}(R)|R|^{\frac{1}{\xi}}}\right). \end{aligned} \quad (\text{S24})$$

Note that this expression is completely independent of σ , as expected in the mean-field limit. For given values of the parameters γ, ρ^*, T and α , the Maxwell construction or the double-tangent construction can be performed numerically, yielding the “liquid” and “gas” values of R , which then yields the coexistence densities with Eq. (S23).

Surface tension and nucleation

The surface tension is computed from the generalized free energy density and the coexistence densities R_g and R_ℓ and reads, see [15, 16],

$$\zeta = \int_{R_g}^{R_\ell} \sqrt{2\kappa(R)\Delta g(R)}dR, \quad (\text{S25})$$

with $\Delta g = \tilde{g}(\rho) - \tilde{g}(R_\ell)$ and $\tilde{g}(R) = g(R) - \mu_0(R_\ell)R$, the free energy density tilted by the chemical potential at phase coexistence. As such, the surface tension ζ depends on the interaction range σ via $\kappa(\rho)$, see Eq. (S16), that ultimately controls the width of the interface between the liquid and the gas. We thus normalize the tension by the length σ in the main text.

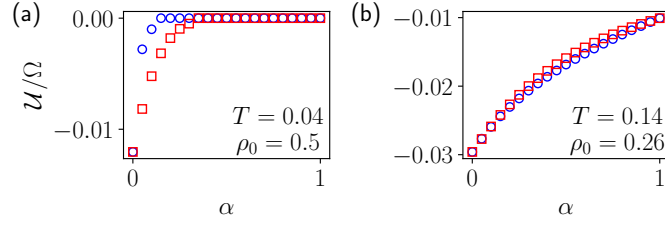


FIG. S1. Evolution of the global utility $\mathcal{U}[\rho] = \int dx u(\phi([\rho], x))\rho(x)$ in the steady state obtained from the numerical resolution of the noiseless PDE ($L = 1000$, $\sigma = 10$) with the level of altruism α for two populations (\circ) and the single population simplification (\square). (a) Settings where individualists sub-optimally aggregate and the phase separation is detrimental. (b) Settings where individualists are not able to aggregate due to noise and the phase separation is beneficial.

To assess the nucleation rate, we need the quasi-potential at the critical radius R_c . Following Ref.[33], the critical radius in $d = 2$ is given by

$$R_c = \frac{\zeta}{\epsilon \Delta R \mu'_0(\rho_g)}, \quad (\text{S26})$$

with $\epsilon = \rho_0 - \rho_g$ the saturation of the homogeneous state in the binodal and with $\Delta R = R_\ell - R_g$. Finally, the quasipotential at the critical radius of a liquid droplet surrounded by the gas reads

$$V(R_c) = \pi \frac{\rho_\ell - \rho_g}{R_\ell - R_g} \frac{\zeta^2}{\epsilon (R_\ell - R_g) \mu'_0(\rho_g)}. \quad (\text{S27})$$

Equivalently, the quasipotential to nucleate a bubble of gas in a liquid is obtained by exchanging the indices $\ell \leftrightarrow g$ in the formula above. In practice, since all quantities are α dependent, the effect of α on the quasipotential is not easily apprehensible.

Impact of altruism on the global utility

In the thermodynamic limit, the coexistence densities given by the binodal curves are sufficient to compute the global utility. In a system of sides of length L , the interface region is indeed sub-dominant and grows as L^{d-1} in contrast with the liquid and gas phases that cover a region scaling as L^d . More generally,

$$\frac{\mathcal{U}}{\Omega} = \frac{\rho_0 - \rho_g}{\rho_\ell - \rho_g} u(\rho_\ell) + \frac{\rho_\ell - \rho_0}{\rho_\ell - \rho_g} u(\rho_g) + O\left(\frac{1}{L}\right), \quad (\text{S28})$$

with Ω the total volume of the system. As naturally expected, this quantity is maximal for $\alpha = 1$, as it is the objective function optimized by all agents, while it is a decreasing function of $1 - \alpha$, see the annotations of Fig. 3.

To get a clearer picture, we plot in Fig. S1 the evolution of this quantity in a noiseless finite size system for the parameter of Fig. S1. Clearly, the ability of altruism to strongly impact the coexistence densities at low temperatures translates in a very rapid increase of the global utility. On the other hand, at higher temperatures when the effect is more progressive, we observe a progressive increase of the global utility once the system is in a phase separated regime.